Springer

KSME

Journal of Mechanical Science and Technology 24 (2) (2010) 471~479
www.springerlink.com/content/1738-494x
DOI 10.1007/s12206-009-1207-5

# Analysis of tensile properties for composites with wrinkled fabric †

Thanh Trung Do and Dong Joo Lee*

*School of Mechanical Engineering, Yeungnam University,*
*214-1, Daedong, Gyeongsan-si, Gyeongsangbuk-do, 712-714, Korea*

(Manuscript Received February 2, 2009; Revised September 30, 2009; Accepted October 13, 2009)

**Abstract**

During the fiber preform loading process of resin transfer moldings (RTMs), fabric layers can be wrinkled in the preform, which affects the quality of the composite. This study considers several wrinkled models with different wrinkled lengths ($L_W$) and different numbers of wrinkled layers in the preform. To study the effects of wrinkling on tensile properties, two matrix materials with different moduli are used to enhance understanding. It is found that the tensile moduli of wrinkled models are lower than those of the normal model, for the same fiber volume fraction ($V_f$). The effects of wrinkling on the tensile modulus increase with the number of layers as well as $V_f$. In addition, the effect of wrinkling with a low-modulus matrix on the tensile modulus is larger than that with a high-modulus matrix in the composite. Based on the failure modes and the stiffness of materials, the failure mechanisms of wrinkled models can be separated into two regimes as a function of wrinkled length, $L_W$, depending on the critical wrinkled length ($L_{WC}$).

*Keywords*: Composites; Resin transfer molding (RTM); Wrinkling; Tensile modulus and strength; Failure mechanisms

## 1. Introduction

Resin transfer molding composites (RTMCs) are being widely used in the manufacture of fiber-reinforced plastic materials because of their applicability in the production of composite materials that are cost-effective and light-weight and that have a high specific strength and a specific stiffness. The manufacture of RTMCs consists of four steps: fiber preform loading; resin injection; curing; and demolding. First, the fiber preform is placed in a closed mold. The mixture of resin and hardener materials is then injected at a low pressure into the mold. After curing, the finished composite is removed from the mold [1-5]. During the preform loading process, wrinkling easily occurs in the fabric preform and can be a source of crack initiation. However, not many studies have been undertaken and published especially on the effects of wrinkling on mechanical properties. Hence, further research is necessary.

Also, laminar composites have some inevitable problems due to the wrinkled pattern for different geometrical structures, stacking sequences and material stiffnesses. Even though the advantages of laminar fabric composites are not proven in terms of the elastic properties, the use of these composites has increased due to many advantages such as the low cost of manufacture, the high fracture toughness, thermodynamic properties and the processing technique. These benefits are related to the current textile technologies, which allow the production of fabrics with many options. The elastic properties modeling can be considered as the first step in the design of new material [6]. However, due to this wrinkling, the mechanical properties of these composites can also be significantly degraded.

The mechanical properties of fiber-reinforced plastics materials have been widely studied for several matrix and fiber materials; studies have focused on the characterization of processing and mechanical properties [7, 8]. Using the three-point bending test, Hobbiebrunken [9] investigated interfacial failure on the basis of experimental and numerical results. He indicated that the interfacial strength must be lower than the matrix strength and showed that the interfacial failure was the dominant failure mechanism. For the same carbon fiber with the same treatment, the interfacial failure was either adhesive (weak interface) or cohesive (strong interface), depending on the matrix system. In addition, some authors have also worked on the effects of the manufacturing and performance of RTMCs on tensile properties. For instance, Holmberg and Berglund [10] studied the problems of the fiber preform of U-beams and tensile failure mechanisms. They concluded that the reinforcement easily led to fabric discontinuity in the preform during preforming and/or mold closuring. This discontinuity caused a problem such as increasing void content of the

† This paper was recommended for publication in revised form by Associate Editor Chongdu Cho
*Corresponding author. Tel.: +82 53 810 2469, Fax.: +82 53 813 3703
E-mail address: djlee@yu.ac.kr

finished composite, etc. [10-12]. Hence, wrinkled fabric in the preform can also occur and affect the quality of the composite.

Using a standard tensile test, this study examines the tensile properties of RTMCs with several wrinkled preform models of K618/R409 and K618/R235 composites. On the basis of an energy method, the analysis of the tensile modulus is performed and then compared with experimental data for understanding the effects of wrinkled patterns and matrix materials. The tensile strength and failure mechanisms of the composites with the wrinkled fabric are analyzed as functions of the wrinkled length, fabric layers and matrix materials. In addition, the shear strength for a critical wrinkled length is determined too.

## 2. Experimental details

The materials prepared for the experiments were polyester resins, R235 and R409, from Sewon Chemical Co. and E-glass woven fabric, K618, from Hankuk Fibers Co. For reducing the curing time, the hardener material of Luperox DDM from Seki Arkema Co. was mixed with the resins, R235 and R409, in a weight ratio of 1:120 and cured at room temperature in a closed mold. The specimens were fabricated by the resin transfer molding process. The basic physical and mechanical properties are given in Table 1.

The specimens used in this study were modeled in accordance with the ASTM D3039-76 standard tensile test with a gage length of $L$ = 100 mm and a rectangular cross-section, which had a thickness of $t$ = 2.1 mm and a width of $b$ = 33.3 mm for the K618/R235 composite and a thickness of $t$ = 2.5 mm and a width of $b$ = 33 mm for the K618/R409 composite. The thickness of laminates was total numbers of plies used to fabricate the specimen. The ends of the specimens were cohesively bonded by the laminated tabs for the load-transfer from the machine grips to the specimens without damage to the specimens, as shown in Fig. 1. The test specimens were cut by an electric band-saw from an original plate of size, 300 mm x 200 mm.

During the preform loading or thermoforming process, a wrinkled fabric preform with different wrinkled lengths can occur. Those affect the mechanical properties and failure mode [10, 11, 13]. To study the effects of wrinkling on the tensile properties, the geometrical structures of the fabric preform types were selected as the following models with different layers and wrinkled lengths as described below (see Fig. 2).

- Model 1 was a normal type. The fabric preform pattern had different numbers of continuous layers, i.e., 2, 4, 6, 8 and 10 layers for the K618/R235 composite and 5, 7 and 9 layers for the K618/R409 composite.
- Models W-1, W-2, W-3 and W-4 were the wrinkled types with 1, 2, 3 and 4 wrinkled layers, respectively. The wrinkled specimens with different numbers of wrinkled layer had the same thickness values. Also, the thickness along the length direction of the specimen was uniform. The ratio of the wrinkled length to the gage length ($L_W/L$) was varied from 0.1 to 0.9.

Table 1. The basic physical and mechanical properties of the resin and fabric.

| Polyester resin | | | | | |
|---|---|---|---|---|---|
| Type | Density (g/cm$^3$) | Viscosity (Poise/25°C) | Curing time at 25°C (min.) | Tensile strength (MPa) | Tensile modulus (GPa) |
| R409 | 1.12 | 1.17 | 7 | 31 | 1.1 |
| R235 | 1.05 | 1.15 | 7 | 36 | 1.3 |
| Plain woven fabric (K618) | | | | | |
| Count (Yarns/In.) | | Density (g/cm$^3$) | Thickness (mm) | Tensile strength (GPa) | Tensile modulus (GPa) |
| Warp | Weft | | | | |
| 18 | 18 | 2.54 | 0.18 | 3.4 | 70 |

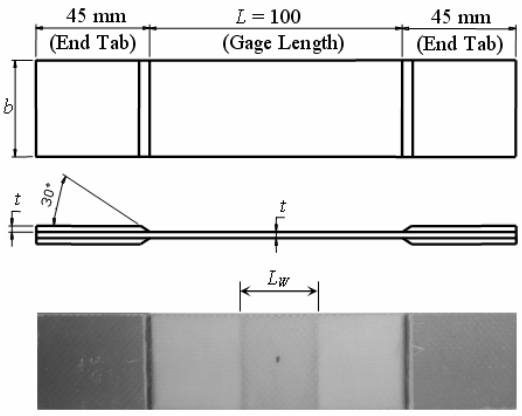


Fig. 1. Configuration of the tensile test specimen.

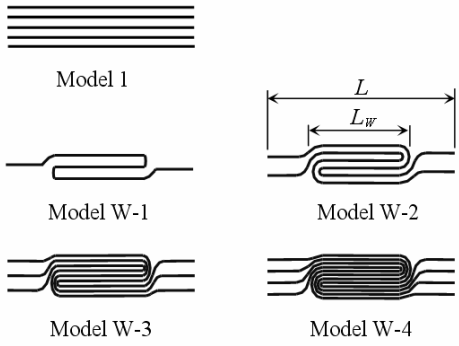


Fig. 2. Fabric preform models.

To examine the tensile properties of selected models, several test specimens were built and preformed. First the end tabs of each specimen were clamped in the grips of the tensile testing machine. Then, the tensile load was applied. The test conditions refer to the ASTM standard [14], and a low loading speed of 3 mm/min. was chosen to fully examine the effects of wrinkling. All tests were done by using a Shimazu testing machine at room temperature and a relative humidity of 50%. The stress-strain curves were recorded from the tensile tests for both the normal and wrinkled specimens. Typically, at least three specimens were used for a single evaluation.

## 3. Results and discussion

### *3.1 Tensile strength*

In this study, the tensile strength is determined from a maximum load and a cross-sectional area of the K618/R409 and K618/R235 composites. In addition, the tensile strength also can be predicted by using the modified rule of mixtures to consider the effects of the fiber volume fraction in RTM composites, as in the following equation [15-17].

$$\sigma_{\max} = C_\sigma \sigma_f V_f' + \sigma_m (1 - V_f') \quad (1)$$

In Eq. (1), $\sigma_m$ and $\sigma_f$ are the tensile strengths of the matrix (36 MPa for R235 and 31 MPa for R409) and fiber (3.4 GPa for K618), respectively, $C_\sigma$ is the fiber-efficiency parameter for the tensile strength, and $V_f'$ is the effective fiber volume fraction.

The fiber volume fraction was determined by using the density of the matrix, fiber and composite. Since the plain woven fabric K618 had the "fiber" symmetry as in woven or cross-plied as $0^o$ and $90^o$ fiber reinforcement, the effective fiber ($V_f'$) as the load carrying fiber was assumed to be only 50% of the fiber in the fabric preform ($V_f$) for better comparison, $V_f' = 0.5V_f$. For various numbers of the continuous layers (which correspond to different effective fiber volume fractions), the tensile strength was determined as the maximum stress of laminate composites for the normal model (Model 1), as shown in Fig. 3. The values predicted through Eq. (1) were in agreement with $C_\sigma = 0.35$ for K618/R235 and $C_\sigma = 0.27$ for K618/R409. These values are due to the interface conditions and the fabric-type reinforcing element. The difference in the tensile strengths between the K618/R235 and K618/R409 composites considerably increased with the number of continuous layers. As expected, the tensile strength of the composite with the high-strength matrix (R235) was larger than that of the composite with the low-strength matrix (R409) for any given fiber volume fraction and the same fiber material (K618). It is clear that the effects of matrix properties, including the density and stiffness, on the tensile strength are reasonable for the different fiber-efficiency parameters.

Fig. 4 shows the tensile strength of wrinkled models with various numbers of wrinkled layers, as a function of the wrinkled length. The tensile strength exhibited two regimes as $L_W/L$ increased, depending on both the fiber volume fraction (through the number of layers) and the matrix property (through the shear strength in the wrinkling section). Since the tensile load always increased with the axial elongation up to the final failure with a loud bang, the tensile strength was determined as the failure strength.

For the first regime (I), where the wrinkled length was smaller than the critical wrinkled length, i.e., $L_W < L_{WC}$, a failure occurred at the interfacial bond of the wrinkling section. The 'critical wrinkled length' is defined as the minimum wrinkled length required for the fiber stress to be equal to the ultimate fiber strength at the middle of the wrinkling section. The

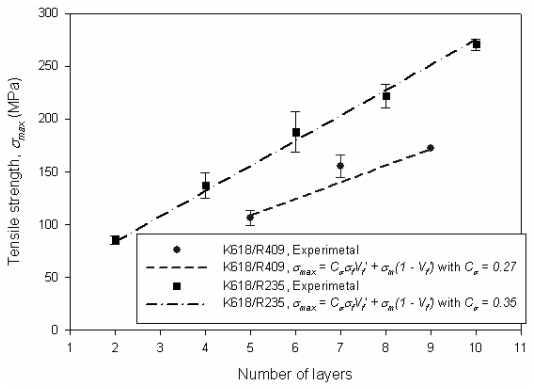


Fig. 3. Tensile strength of the normal model (Model 1) as a function of the number of layers.

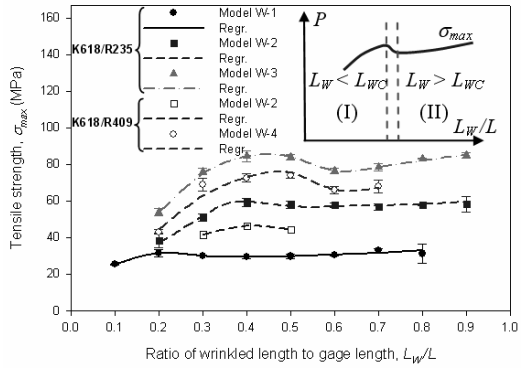


Fig. 4. Variation of the tensile strength of wrinkled models with the relative wrinkled length.

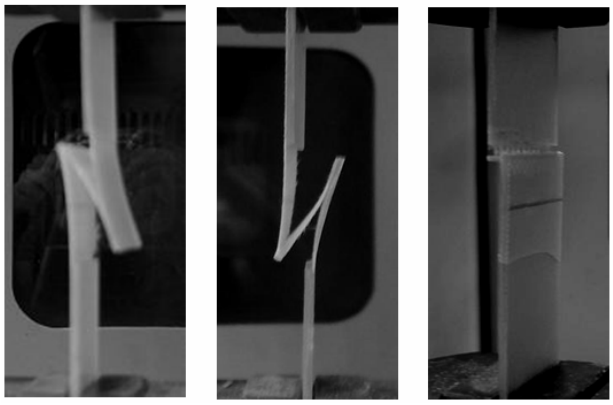

(a) Model W-3 (b) Model W-2 (c) Model W-1

Fig. 5. The failure shapes of K618/R235 specimens when $L_W/L = 0.3$.

interfacial bond [15, 16, 18, 19] failed before the fibers achieved their potential strength, as shown in Figs. 5(a) and 5(b). The main causes of those failures were due to Mode I (opening failure) and Mode II (pulling failure). The failures can be analyzed as follows.

Consider an infinitesimal length $dL_W$ that belongs to $L_W$, as shown in Fig. 6. Since the matrix has a much lower tensile modulus and strength than the fiber, the longitudinal strain at failure in the matrix is larger than that in the fiber [15]. If a

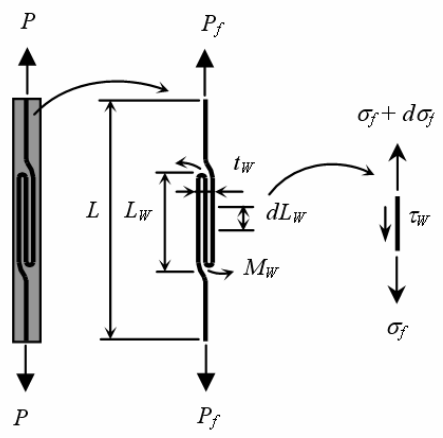


Fig. 6. Wrinkled model used in the analytical study.

perfect bond is assumed for each fabric layer, the difference in longitudinal strains creates the shear stress and moment at the wrinkling section, when $L_W < L_{WC}$.

The force equilibrium equations in the loading direction as shown in Fig. 6 are:

$$bt_f\left(\sigma_f + d\sigma_f\right) - bt_f\sigma_f - 2b(dL_W)\tau_W = 0$$

$$\text{and } \frac{d\sigma_f}{dL_W} = \frac{2\tau_W}{t_f} \tag{2}$$

For simplicity of analysis, it is often assumed that the interfacial shear stress is a constant; thus,

$$\sigma_f = \frac{2\tau_W}{t_f} L_W \tag{3}$$

In Eqs. (2) and (3), $b$ is the width of the specimen, $\tau_W$ is the interfacial shear stress, $\sigma_f$ is the longitudinal stress of the fiber, and $t_f$ is the thickness of a layer.

When the composite lamina contains wrinkled layers that can be assumed to be discontinuous fibers, the fiber stress is not uniform. It is zero at the ends of the wrinkling section and linearly builds up to the maximum value at the central portion of the fiber [15, 16]. The maximum fiber stress due to the shear that can be achieved at a given load is:

$$\left(\sigma_{fs}\right)_{\max} = \frac{2\tau_W}{t_f}\frac{L_W}{2} = \frac{\tau_W}{t_f} L_W \tag{4}$$

In addition, the moment ($M_W$) exists in this case and the maximum fiber stress due to the moment is described by:

$$\left(\sigma_{fm}\right)_{\max} = \frac{1}{2}\frac{M_W}{I}\frac{t_W}{2} = \frac{3}{2}\frac{P_f}{bt_W}$$

$$\text{where } M_W = P_f\frac{t_W}{2} \text{ and } I = \frac{bt_W^3}{12} \tag{5}$$

In Eq. (5), $t_W$ is the thickness of the wrinkled fabric (Fig. 6), $I$ is the moment of inertia of the wrinkling section, and $P_f$ is the tensile load of the fiber at failure.

Therefore, the total maximum fiber stress due to the shear and the moment can be derived from Eqs. (4) and (5) as:

$$\sigma_{fu} = \frac{\tau_W}{t_f} L_W + \frac{3}{2}\frac{P_f}{bt_W} \tag{6}$$

A critical wrinkled length can be calculated from Eq. (6) as:

$$L_{WC} = \left(\sigma_{fu} - \frac{3}{2}\frac{P_f}{bt_W}\right)\left(\frac{t_f}{\tau_W}\right) \tag{7}$$

In Eq. (7), $L_{WC}$ is the critical wrinkled length that is required for the fiber stress to be equal to the ultimate fiber strength ($\sigma_{fu}$) at the middle of the wrinkling section.

Based on the rule of mixture [15-17], the tensile strength of the composite with the wrinkled preform for a boundary condition of $L_W < L_{WC}$ can be given by:

$$\sigma_{\max} = \left(\frac{\tau_W}{t_f} L_W + \frac{3}{2}\frac{P_f}{bt_W}\right)V_f' + \sigma_m'(1 - V_f') \tag{8}$$

In Eq. (8), $V_f'$ is the effective fiber volume fraction, $V_f' = 0.5V_f$, $\sigma'_m$ is the matrix stress at the instant of composite failure, and $P_f$ is the tensile load of the fiber that can predicted from the tensile loads of the composite and the matrix at the failure of the composite. Then, the tensile strength of wrinkled models for regime (I) can be determined through Eq. (8).

The opening and pulling failures did not occur when the wrinkled length reached a value that was larger than the critical wrinkled length as $L_W > L_{WC}$. In this case, failures of the composites were due to breaking fibers for the second regime (II), as shown in Fig. 5(c). The maximum fiber stress and stress concentration [15, 16, 20] at both ends of the wrinkling section were the main causes for the failure strength.

Therefore, when the wrinkled length is larger than the critical wrinkled length ($L_W > L_{WC}$), the maximum fiber stress of the non-wrinkling section may reach the ultimate fiber strength ($\sigma_{fu}$) and the tensile strength of the composite is then given by:

$$\sigma_{\max} = \sigma_{fu}\left(1 - \frac{L_W}{L}\right)V_f' + \sigma_m'(1 - V_f') \tag{9}$$

In Eq. (9), $L$ (= 100 mm) is a gage length of the specimen, $V_f'$ is the effective fiber volume fraction, and $\sigma'_m$ is the matrix stress at the instant of composite failure.

In general, the composites become much stronger and stiffer under tension because the shear factor decreases as the wrinkled length increases. This is a reason why the tensile strength was always increasing with the wrinkled length for both the regimes. However, due to the geometrical structure of curved

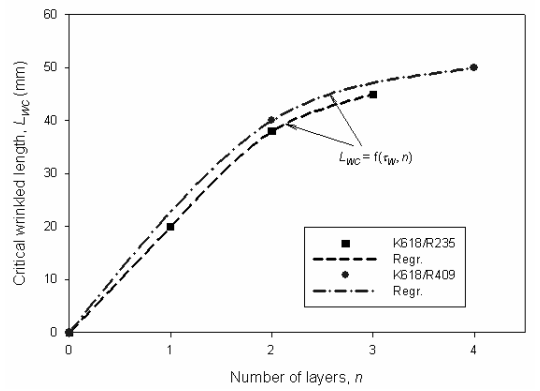


(a) Experimental results

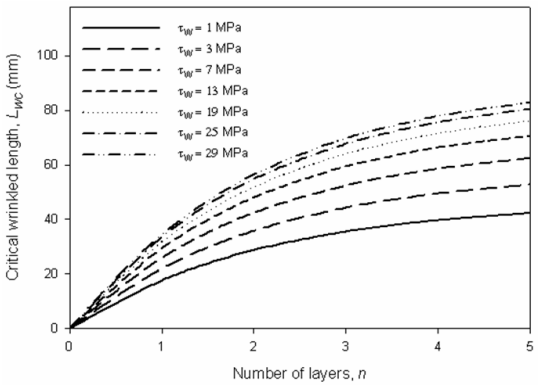


(b) Predicted results

Fig. 7. The experimental and predicted results of the critical wrinkled lengths.

fibers at both ends of the wrinkling section, the redistribution of the load-transfer and stress-transfer [21] at the wrinkling ends occurred easily. Transferring the tensile strength from regime (I) to regime (II) is reasonable as described in Fig. 4. Based on the experimental results, the critical wrinkled lengths for the K618/R235 and K618/R409 composites were obtained as shown in Fig. 7(a). To use this data for designing with composites, it is necessary to generalize this behavior, as a function of the shear strength ($\tau_W$) and the number of layers ($n$), as described by the following equation.

$$L_{WC} = 40n^{0.07}\tau_W^{0.2}\left(1-e^{-0.58n}\right) \tag{10}$$

where n ≥ 0, integer.

The shear strengths for the K618/R235 and K618/R409 composites were determined from Eq. (8), when $L_W = L_{WC}$, and are described in Table 2. The results showed that the shear strength was larger for the matrix having high-strength (R235) [9]. Also, the shear strength increased about 10% with increasing one layer in the wrinkled preform. It is believed that the better bonding between the layers when increasing the wrinkled layer in the prefom is the reason. The higher fiber volume fraction needed the higher pressure for permeability that can be expected from the same thickness of its composites. As

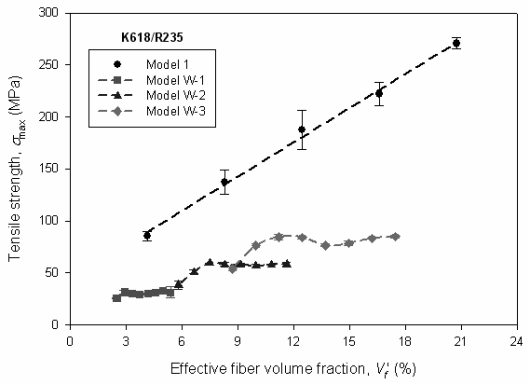


Fig. 8. Tensile strength versus $V_f'$ for K618/R235.

expected, for given properties of the matrix, fiber and composite, the shear strength at a certain wrinkled length can be determined under a given tensile load. The shear strength must be smaller than matrix strength [9]. In addition, the critical wrinkled length also can be predicted from the given values of the shear strength and the number of layers (Fig. 7(b)). This prediction can be used as a design tool in the case of wrinkled or discontinuous fabric composites.

Fig. 8 compares the tensile strengths between the normal and wrinkled models vs. $V_f'$ for the K618/R235 composite. Due to the effects of the wrinkled pattern, which is assumed as constituting discontinuous fibers, the tensile strengths of wrinkled models were smaller than those of the normal model. The load-transfer and stress-transfer [15, 16, 21] occurred for the wrinkled layers that can be assumed as discontinuous fibers. In addition, the effects of the load-transfer and stress-transfer were much larger when the number of wrinkled layers in the preform increased. The maximum fiber stress at the ends of the wrinkling section reached the ultimate fiber strength. In turn, that meant that, as a function of fiber volume fraction, the tensile strengths of the wrinkled models with a larger number of layers were much smaller than those of the normal model.

### *3.2 Tensile modulus*

The tensile modulus can be determined on the basis of a stress-strain curve from the experimental data. In addition, to consider the effect of the fiber in the composite, the tensile modulus can also be predicted by using the modified rule of mixtures [15-17].

$$E = C_E E_f V_f' + E_m(1-V_f') \tag{11}$$

In Eq. (11), $E_m$ and $E_f$ are the tensile moduli of the matrix (1.3 GPa for R235 and 1.1 GPa for R409) and fiber (70 GPa for K618), respectively. $C_E$ is the fiber-efficiency parameter for the tensile modulus, and $V_f'$ is the effective fiber volume fraction.

Fig. 9 shows the tensile moduli of the K618/R235 and K618/R409 composites vs. $V_f'$ where $V_f' = 0.5V_f$. The values

Table 2. Calculated shear strength ($\tau_W$), derived from Eq. (8), at the critical wrinkled length ($L_{WC}$).

| Type | Model | $L_{WC}$ (mm) | $\sigma_c$ (MPa) | $\sigma_m$' (MPa) | $P_f = P_c - P_m$' (kN) | $\tau_W$ (MPa) | $\sigma_c/\tau_W$ |
|---|---|---|---|---|---|---|---|
| K618/R235 | W-1 | 20 | 31.429 | 19 | 1.211 | 3.7 | 8.49 |
| | W-2 | 38 | 61.162 | 24 | 3.462 | 4.1 | 14.92 |
| | W-3 | 45 | 83.966 | 29 | 5.408 | 4.3 | 19.53 |
| K618/R409 | W-2 | 40 | 46.3 | 21 | 2.882 | 3.3 | 14.03 |
| | W-4 | 50 | 73.044 | 26 | 5.734 | 3.7 | 19.74 |

where $P_f$, $P_c$, and $P_m$' are the tensile loads of the fiber, composite, and matrix, respectively; $\sigma_c$ and $\sigma_m$' are the tensile strengths of the composite and matrix at failure, respectively.

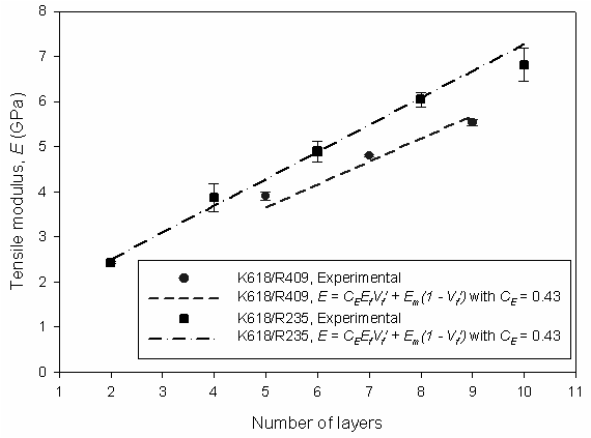


Fig. 9. Tensile modulus of Model 1.

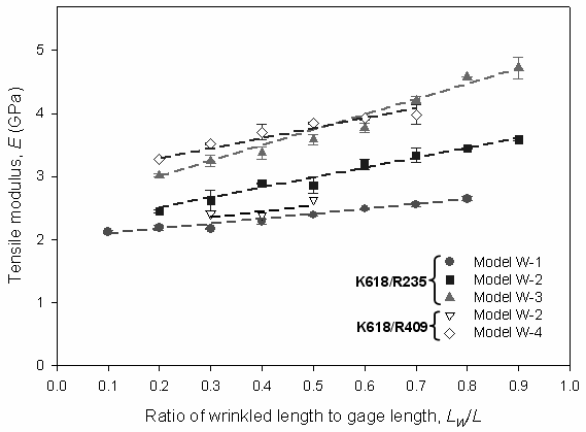


Fig. 10. Tensile moduli of the wrinkled models.

of $V_f$ were determined by using the densities of the matrix, fiber and composite. Also, in this comparison, half the measured $V_f$ is used since the effective fibers are assumed to be only 50% of the fibers in the fabric preform. The modulus that is calculated through Eq. (11) is well-matched with the fiber-efficiency parameter of 0.43 instead of 1 for both the K618/R235 and K618/R409 composites. It is believed that this was due to not only the imperfect interface, matrix viscosity and fabric type, which were not easy to wet thoroughly, but also the nature of the woven fabric. The differences in the tensile moduli of the K618/R235 and K618/R409 composites were larger as the number of continuous layers in the preform increased. It is clear that the difference in the effects of the matrix on the tensile modulus was small when $V_f$' was small, but became larger when $V_f$' increased.

For different wrinkled models with various wrinkled lengths ($L_W$), the tensile moduli of RTMCs in the form of K618/R235 and K618/R409 laminate specimens were determined and are described in Fig. 10. It is found that the tensile modulus increased linearly with $L_W$. The composite with the matrix of a high-modulus has a steeper slope as the fiber volume fraction increases. As expected, the wrinkled models with a larger number of layers or a higher fiber volume fraction in the preform have a larger tensile modulus for both matrix materials.

The comparison of the tensile moduli between the normal model and wrinkled models vs. $V_f$' is shown in Fig. 11. Since the load-transfer of the wrinkled layers, which were assumed to be discontinuous fibers, occurred and the longitudinal strain

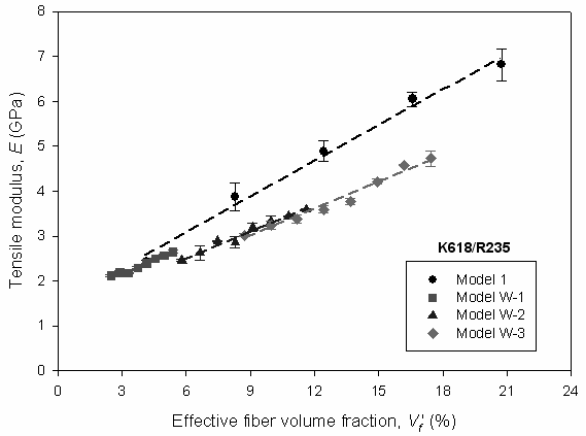


Fig. 11. Comparison of the tensile moduli of the K618/R235 composites.

of the wrinkling section was larger than that of the normal section during the elastic period, the tensile moduli of the wrinkled models were always smaller than those of the normal model as functions of fabric layers. In addition, those effects were much larger when the number of wrinkled layers in the preform increased. This implies that the tensile moduli of the wrinkled models with many layers were much smaller than those of the normal model as a function of fiber volume fraction. It is observed that the difference is below 0.3 GPa when the preform has the minimum number (i.e., one) of wrinkled layers with a small $V_f$', which is below 5%. In addition, at the same $V_f$', the tensile moduli for the wrinkled models were

almost the same regardless of the differences in the number of layers and the wrinkled length in the preform. It is clear that the tensile moduli of the wrinkled models mostly depended on the fiber volume fraction, matrix and fiber types, even though the number of layers and wrinkled lengths varied in the fabric preform.

Fig. 12 shows the differences in the tensile moduli between the normal and wrinkled models for a high-modulus matrix in the composite (1.3 GPa for R235) and a low-modulus matrix in the composite (1.1 GPa for R409) as a function of $V_f'$, where both contain the same fiber material (K618). There was a larger difference in the tensile modulus between Model 1 and Model W-2, for both composites, as $V_f'$ increased. In addition, the slope of the difference for the K618/R235 composite was smaller than that for the K618/R409 composite. It is clear that the effect of a low-modulus matrix on the tensile moduli of wrinkled models was larger than that of a high-modulus matrix, as a function of fiber volume fraction in the composite.

Based on an energy method, the analytical elastic elongation, $\lambda$, is:

$$\lambda = \frac{2U}{P} = \frac{P}{A}\left[\frac{L - L_W}{E_1} + \frac{L_W}{E_2}\right] \tag{12}$$

In Eq. (12), $E_1$ and $E_2$ are the moduli for the non-wrinkling and wrinkling sections, respectively. They can be predicted from the normal model (Model 1) with a given number of continuous layers.

Due to the effects of wrinkling, the analytical elastic elongation, $\lambda$, differs from the experimental result ($\lambda$*). It can be described as $\lambda^* = \alpha\lambda$. The value of $\alpha$ is a 'damage' parameter that arises from wrinkling.

It is assumed that $E_1$ and $E_2$ are the constant values, which are predicted from the normal preform type (Model 1). For K618/R235, $E_1$ are 2.1 GPa, 2.5 GPa and 3.2 GPa, and $E_2$ are 3.2 GPa, 4.8 GPa and 6.5 GPa for Models W-1, W-2 and W-3, respectively. Similarly, for K618/R409, $E_1$ are 2.4 GPa and 3.6 GPa, and $E_2$ are 4.2 GPa and 7 GPa for Models W-2 and W-4, respectively.

Fig. 13 shows the experimental and analytical results of the elastic elongation at $P$ = 0.86 kN vs. $L_W/L$ for various wrinkled models. For K618/R235, the value predicted through Eq. (12) is in good agreement with $\alpha$ = 1.1 for Model W-1 (one layer), $\alpha$ = 1.18 for Model W-2 (two layers), and $\alpha$ = 1.24 for Model W-3 (three layers). For K618/R409, $\alpha$ = 1.19 for Model W-2 (two layers) and $\alpha$ = 1.36 for Model W-4 (four layers). Due to the curved fibers at the ends of the wrinkling section, the axial elongations of the wrinkled models were larger than those of the normal model during elastic tensile loading. In addition, the load-transfer and stress-transfer [15, 16, 21] occurred for wrinkled types in the manner of discontinuous fibers. The effects of wrinkling clearly can be seen though the wrinkle-damage parameter, $\alpha > 1$, which describes the effects of wrinkling patterns as well as the effects of matrix materials on the elastic moduli of the composites. The wrinkle-damage parameter increased with the number of layers, as shown in Fig. 14. The slope for the low-modulus matrix (R409) was steeper than that of the high-modulus matrix (R235) in the α-n graph. This means that the matrix with the lower modulus is more sensitive to wrinkling with regard to the tensile modulus for the same fiber material and fiber volume fraction in the composite.

In general, the results show that the wrinkle-damage parameter increases with the number of layers. This is because of a greater load-transfer, stress-transfer and longitudinal

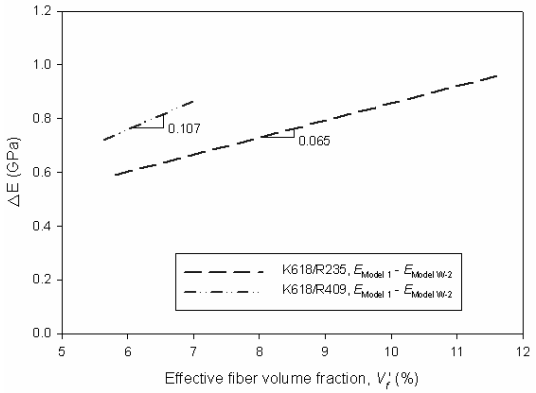


Fig. 12. Difference in the tensile modulus between the normal and wrinkled models.

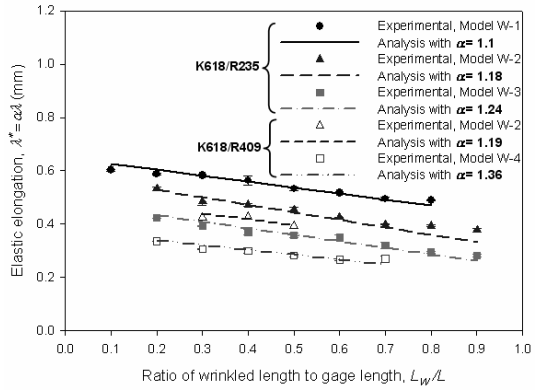


Fig. 13. Experimental and predicted elastic elongation results of the wrinkled models at $P$ = 0.86 kN.

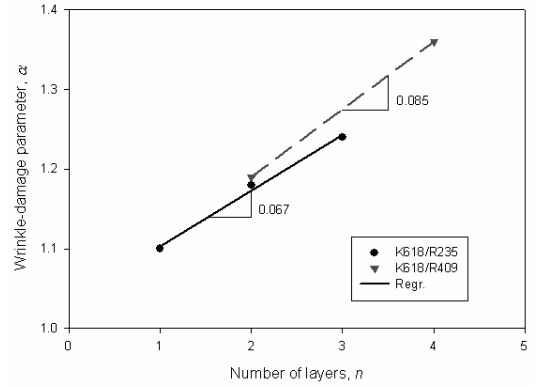


Fig. 14. Wrinkle-damage parameter versus the number of layers.

strain when the number of wrinkled layers in the preform increases. Therefore, a low elastic modulus in these composites is reasonable. The wrinkle-damage parameters for wrinkled models with a high-modulus matrix are smaller than those for models with a low-modulus matrix in the composite. This means that these parameters depend not only on the number of layers but also the matrix material that is related to the stress concentration [15, 16, 20] at the ends of the wrinkling section.

## 4. Conclusions

Based on this study, the following conclusions can be drawn.

- The tensile modulus and strength as yielded by experiments are well-matched with the values that are predicted through the modified rule of mixtures with the fiber-efficiency parameters of 0.43 and 0.27 for K618/R409, and 0.43 and 0.35 for K618/R235, respectively.
- The tensile modulus of the composite with a high-modulus matrix is much larger than that of the composite with a low-modulus matrix when the fiber volume fraction is increased.
- The tensile modulus and strength increase with the fiber volume fraction. However, the results of the normal model are quite bigger than those of the wrinkled models. This is due to the effect of wrinkling, which is assumed to constitute discontinuous fibers.
- The tensile strength of wrinkled models has two failing mechanisms as a function of the wrinkled length. Due to the failure modes and the stiffness of the matrix, the failure strengths of regimes (I) and (II) are mainly due to the matrix and fiber failures, respectively.
- As expected, for given properties of the matrix, fiber and composite, the shear strength at a certain wrinkled length can be determined under the tension.
- Due to effects of the wrinkling, such as the load-transfer and shear stress, the longitudinal strain of wrinkled models is larger than that of the normal model, as a function of the fiber volume fraction.

## Acknowledgment

This research was supported by a Research Grant from Yeungnam University in 2008.

## References

[1] B. Yang, V. Kozey, S. Adanur and S. Kumar, Bending, compression, and shear behavior of woven glass fiber–epoxy composites, *Composites Part B* 31 (2000) 715-721.

[2] R. J. Day, P.A. Lovell and A. A. Wazzan, Toughened carbon/epoxy composites made by using core/shell particles, *Composites Science and Technology* 61 (2001) 41-56.

[3] J. M. Lawrence, P. Fried and S. G. Advani, Automated manufacturing environment to address bulk permeability variations and race tracking in resin transfer molding by redirecting flow with auxiliary gates, *Composites Part A* 36 (2005) 1-14.

[4] M. Deleglise, C. Binetruy and P. Krawczak, Solution to filling time prediction issues for constant pressure driven injection in RTM, *Composites Part A* 36 (2005) 339-344.

[5] A. Cheung, Y. Yu and K. Pochiraju, Three-dimensional finite element simulation of curing of polymer composites, *Finite Elements in Analysis and Design* 40 (2004) 895-912.

[6] J. Bystrom, N. Jekabsons and J. Varna, An evaluation of different models for prediction of elastic properties of woven composites, *Composites Part B* 31 (2000) 7-20.

[7] G. Swaminathan, K. N. Shivakumar and M. Sharpe, Material property characterization of glass and carbon/vinyl ester composites, *Composites Science and Technology* 66 (2006) 1399-1408.

[8] Y. Zhou, F. Pervin, V. K. Rangari and S. Jeelani, Fabrication and evaluation of carbon nano fiber filled carbon/epoxy composite, *Materials Science & Engineering A* 426 (2006) 221-228.

[9] T. Hobbiebrunken, M. Hojo, T. Adachi, C. De Jong and B. Fiedler, Evaluation of interfacial strength in CF/epoxies using FEM and in-situ experiments, *Composites Part A* 27 (2006) 2248-2256.

[10] J. A. Holmberg and L. A. Berglund, Manufacturing and performance of RTM U-beams, *Composites Part A* 28 (1997) 513-521.

[11] K. Potter, B. Khan, M. Wisnom, T. Bell and J. Stevens, Variability, fiber waviness and misalignment in the determination of the properties of composite materials and structures, *Composites Part A* 39 (2008) 1343-1354.

[12] H. Huang and R. Talreja, Effects of void geometry on elastic properties of unidirectional fiber reinforced composites, *Composites Science and Technology* 65 (2005) 1964-1981.

[13] R. K. Pandey and C. T. Sun, Mechanisms of wrinkle formation during the processing of composite lamintes, *Composites Science and Technology* 59 (1999) 405-417.

[14] *Annual book of ASTM standards*, 8 (1995).

[15] P. K. Mallick, *Fiber-reinforced composites*, Marcel Dekker, New York, USA, (1998).

[16] R. M. Jones, *Mechanics of composite materials*, McGraw-Hill Kogakusha, Tokyo, Japan, (1975).

[17] P. T. Curtis, M. G. Blade and J. E. Bailey, The stiffness and strength of polyamide thermoplastic reinforced with glass and carbon fiber, *J. of Mat. Sci.* 13 (1978) 377-390.

[18] H. Lanting and J. K. Spelt, Shear fracture of adhesively-bonded rigid elements, *Composites Part B* 28 (1997) 319-329.

[19] L. K. Jain and Y. W. Mai, Analysis of resin-transfer-moulded single-lap joints, *Composites Science and Technology* 59 (1999) 1513-1518.

[20] L. Tong and G. P. Steven, A numerical study on stresses in resin transfer moulding lap joints reinforced with transverse stitching, *Composite Structures* 36 (1996) 91-100.

[21] G. Kelly, Quasi-static strength and fatigue life of hybrid

(bonded/bolted) composite single-lap joints, *Composite Structures* 72 (2006) 119-129.

**Thanh Trung Do** received his B.S. in Mechanical Engineering from University of Technical Education HoChiMinh City in Vietnam on March 2000. He then received his M.S. degree on September 2003 and Ph.D. degree on August 2009 from Yeungnam University, Korea, where he is currently post-doctoral fellow. He is also member of University of Technical Education HoChiMinh City, Vietnam. His research interests focus on polymer matrix composites and experimental mechanics. His e-mail address is: dttrung@ynu.ac.kr.

**Dong Joo Lee** received his B.E. in Mechanical Engineering from Yeungnam University, Korea, in 1979. He then received his M.S. and Ph.D. degrees from University of Massachusetts at Amherst in 1983 and 1987, respectively. Between 1987 and 1992, he was a research scientist at Honeywell Inc. in N.J. He is currently a Professor at the School of Mechanical Engineering at Yeungnam University. His research interests focus on polymer matrix composites, experimental mechanics and smart materials.